Low Damping of Micron Capillary Waves on Superfluid ^{4}He

P. Roche,[1] G. Deville,[1] K. O. Keshishev,[2] N. J. Appleyard,[1] and F. I. B. Williams[1]

[1]*Laboratoire de la Matière Condensée Quantique, Service de Physique de l'Etat Condensé, Direction des Sciences de la Matière, Centre d'Etudes de Saclay, 91191 Gif sur Yvette, France*

[2]*Kapitza Institute for Physical Problems, Russian Academy of Sciences, Kosygina ul. 2, 117334 Moscow, Russia*

(Received 14 October 1994; revised manuscript received 28 August 1995)

Capillary waves (ripplons) in the wavelength range 3.3–20 μm on a superfluid ^{4}He layer of continuously controllable thickness are generated and detected with coplanar interdigital capacitors. In the bulk limit, the waves propagate over several centimeters at low temperature and the attenuation factor is compatible with a T^4 power law in the temperature interval 300–700 mK. The damping is about 6 orders of magnitude smaller than previous theoretical estimates of ripplon-ripplon scattering. The results point instead to scattering of ripplons by phonons, in accord with a revised calculation.

PACS numbers: 67.40.Pm, 68.10.–m

Capillary waves (ripplons in quantum language) on the surface of bulk superfluid helium seem to be well described as irrotational excitations in a nonviscous, incompressible fluid, at least for wavelengths well in excess of the interatomic spacing [1]. The dispersion relation has been confirmed experimentally for frequencies from 5 kHz to 300 MHz [2–7]. There is, however, a strong discrepancy between theory and experiment concerning damping. The measured linewidths of composite modes involving submicron ripplons coupled to an electron lattice [7] set an upper bound on ripplon damping, which is 2 orders of magnitude *below* accepted theoretical estimates, calculated from the kinetic three-ripplon interaction [8–10]. The sense and the magnitude of this discrepancy points to a serious lack of understanding.

To be sure that the fault does not lie with the interpretation of the experimental data, we have designed an experiment to measure the intrinsic damping of ripplons directly. These new measurements show an even greater discrepancy with existing theory. A reformulation of the theory [11], however, suggests that this arises from a failure to take proper account of the surface boundary condition.

The method developed allows continuous electrical control of the film thickness and so lends itself to studying effects from the bulk to the van der Waals limit, where the excitations should properly be considered as third sound waves. This interesting aspect has not, however, been pursued in full detail here.

The experiments are done on a superfluid layer of helium above a horizontal array of interdigitated electrodes. The liquid is thus manipulated and monitored by means of the dielectric ponderomotive effect. Film thickness is set by a dc voltage; surface waves are generated by an ac voltage and are detected by ac capacitance variation.

The experimental cell is shown in Fig. 1. Three coplanar interdigital capacitors (IDC's) A, B, and C, are patterned by photolithography from a 200 Å layer of chromium on a plane quartz substrate in a way that maintains geometrical periodicity across the three arrays. Each capacitor consists of interlocking fingers of length 2 mm, each being of 10 μm width and separated from its neighbor by 10 μm (denoted IDC10 with repeat distance $\lambda_0 = 40$ μm). A 5 μm/5 μm configuration (IDC5 with $\lambda_0 = 20$ μm) was also used. The total number of fingers in a capacitor of length L is $2L/\lambda_0 = N = 50$, 100, or 150.

Film thickness control.—When the structures are biased with a constant voltage $V_{\rm dc}$, the electric field around the fingers attracts the dielectric helium. The equilibrium thickness $d(x)$ of liquid above the capacitors satisfies [12]

$$(h + d) - \frac{(\varepsilon - 1)\varepsilon_0}{2\rho g}(\varepsilon E_n^2 + E_t^2) - \frac{\kappa^4}{d^3} - \frac{\sigma}{\rho g}\nabla_{x,y}^2 d = 0. \quad (1)$$

E_n and E_t are the normal and tangential components of electric field just below the liquid surface, g the acceleration due to gravity, ρ and ε the helium density and dielectric constants, and σ its surface tension ($\rho = 145$ kg m^{-3}, $\varepsilon = 1.056$, $\sigma \approx 0.378$ mJ m^{-2} at $T = 0$ K). The parameter κ, describing the substrate to liquid helium van der

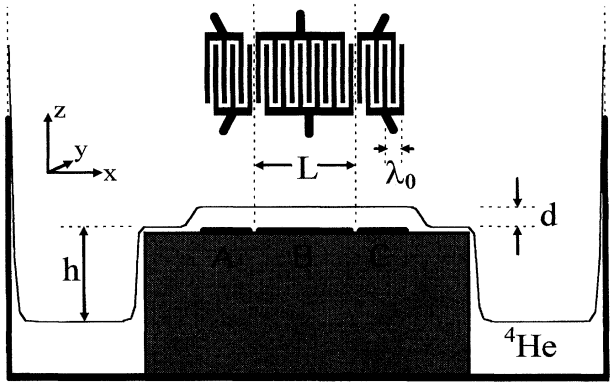

FIG. 1. Schematic view of the experimental cell. The three interdigital capacitors A, B, and C are $h \sim 8$ mm above the free ^{4}He surface. The inset shows their topology.

 0031-9007/95/75(18)/3316(4)$06.00

Waals (vdW) interaction, is approximately 0.7 μm; h is the effective distance to the bulk helium surface below the capacitor plane (typically $h \sim 8$ mm). As $\varepsilon - 1 \ll 1$, we simplify $(\varepsilon E_n^2 + E_t^2)$ to E^2.

The periodic potential produced by the IDC may be expressed in terms of the fundamental wave vector $k_0 = 2\pi/\lambda_0$ by $V = \sum_{p=0} V_p \sin((2p+1)k_0 x) e^{-(2p+1)k_0 z}$, from which we may write the electric field intensity to order V_2:

$$E^2 = k_0^2(V_0^2 + 9V_1^2 e^{-4k_0 z} + 25V_2^2 e^{-8k_0 z})e^{-2k_0 z} + k_0^2(6V_0V_1 + 30V_1V_2 e^{-4k_0 z})e^{-4k_0 z}\cos(2k_0 x) + k_0^2(10V_0V_2)e^{-6k_0 z}\cos(4k_0 x) + \cdots. \quad (2)$$

The coefficients V_p are determined by the basis cell of the structures. For finger width equal to separation, $V_{2n+1} = 0$ [13]. The first term in (2) induces a uniform increase in the equilibrium depth d_0 of liquid, determined principally by a bias voltage V_{dc}. A typical scan of V_{dc} changes the depth from the vdW film thickness (~400 Å) to about $\lambda_0/8$. The subsequent terms in (2) generate a spatially periodic surface deformation $d(x) = d_0 + \sum \zeta_n \cos(2nk_0 x)$.

Figure 2 shows a fixed frequency bridge capacitance measurement of an IDC10 biased with V_{dc} at 200 mK. At $\omega/2\pi = 10$ kHz, a smooth variation is seen on sweeping V_{dc}. The form of this curve is a universal function of d_0/λ_0, allowing us to construct $d_0(V_{dc})$, as shown on the vertical axis. This is cross-checked against a direct

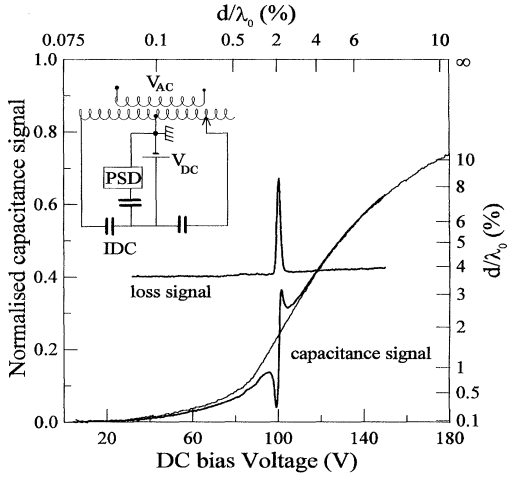

FIG. 2. Experimental signal in an IDC10 ($\lambda_0 = 40$ μm) impedance measurement. The inset shows the capacitance bridge configuration with bias V_{dc}. The light trace is the measured capacitance variation at 10 kHz for $0 < V_{dc} < 180$ V, normalized to the large depth asymptote. The heavy traces are the in-phase and quadrature signals at 82 kHz, showing resonant behavior associated with ripplon generation. Depth deduced from capacitance variation is indicated on the right scale and depth calculated from (1) and (2) on the upper scale.

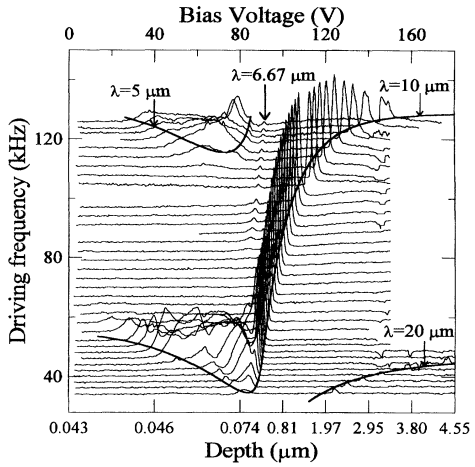

FIG. 3. Predicted resonance frequencies $\omega/2\pi$ vs V_{dc} and a set of experimental signals for an IDC10. The heavy lines show the ripplon resonance condition $k(\omega, d) = 2k_0$, $4k_0$, and $8k_0$ calculated from the dispersion relation (3) using the depth scale deduced from (1) and (2). A sequence of constant frequency experimental absorption (quadrature signal) traces are superimposed. Because of the hierarchy of the V_p, the modes with $k = 4nk_0$ are more readily excited and detected than the $k = 2(2n+1)k_0$ modes.

calculation from Eqs. (1) and (2), shown on the horizontal axes of Figs. 2 and 3; agreement is within 100 Å or 2%.

Ripplon generation and detection.—Irrotational excitations of an inviscid incompressible fluid of depth d propagate according to the dispersion relation,

$$\omega^2(k) = (\rho g' + \sigma k^2)\frac{k\tanh(kd)}{\rho}, \qquad g' = g\left[1 + 3\frac{\kappa^4}{d^4} - \frac{(\varepsilon - 1)\varepsilon_0}{2\rho g}\frac{\partial E^2}{\partial z}\Big|_{z=d}\right], \quad (3)$$

where g' is the gravitylike term, which includes vdW and electrostrictive forces.

The addition of an ac signal $V_{ac}e^{-i\omega t}$ to the bias voltage ($V_{ac} \sim 0.2V_{rms} \ll V_{dc}$) produces a periodic pressure $p(x,t) \sim \frac{1}{2}(\varepsilon - 1)\varepsilon_0 e^2(d,x)e^{-i\omega t}$ on the liquid surface, due to the oscillatory component $e^2(z,x)e^{-i\omega t}$ in (2). This can be used to launch waves $\zeta(u,t) = \zeta(k)e^{i(ku-\omega t)}$, where $k = k(\omega)$ in (3). The amplitude $\zeta(k) \propto \int p(x,t)e^{-i(kx-\omega t)}dx$ will show a resonant response as $k \to 2nk_0$, due to constructive interference between waves from different fingers.

The waves are detected by a reciprocal effect. The presence of liquid above the structure changes its capacitance by $\delta C \approx (\varepsilon - 1)[\int\int^{d(x,t)} |E(z,x)|^2 dz\, dx]/V_{dc}^2$, and the passage of a wave adds a time-dependent component $C(t) \approx (\varepsilon - 1)\zeta(k)e^{-i\omega t}[\int e^{iku}|E(d,u)|^2 du]/V_{dc}^2$. Again, this has resonances as $k \to 2nk_0$.

The effect of the resonance on the impedance of the structure can be seen in the capacitance measurement

at $\omega_{\rm exp}/2\pi = 82$ kHz in Fig. 2 over a narrow interval around $V_{\rm dc} = 100$ V; the phase of the signal allows us to distinguish anomalous dispersion from absorption. The horizontal traces of Fig. 3 constitute a full set of such data; the absorptive part of the signal is shown for a series of fixed frequency sweeps. The resonances correspond with the condition $\omega_{\rm exp} = \omega(k, d_0)$ of the dispersion relation, with $k = 2k_0, 4k_0, 6k_0, \ldots$, the calculated loci of which are shown as heavy lines. The agreement between data and calculated frequencies indicates that the different forces involved in Eqs. (1) and (3) are satisfactorily taken into account. The frequency minimum shows the crossover to the vdW limit. Analysis of the frequency asymptote yields $\sigma = 0.379 \pm 0.004$ mJ m^{-2} at 200 mK [14].

Ripplon attenuation.—The principal object of the present report is to determine linear response ripplon damping in the bulk limit. This can be found either from the linewidth of a ripplon emission resonance in the transmitter impedance or from the reduction in wave amplitude measured by a passive receiver after propagation from a distant transmitter.

The shape of the emission line is determined by interference of waves across the structure. It is broadened, relative to the form for an ideal structure, by imperfect correlation and by temperature-dependent intrinsic wave attenuation. The measured linewidth as a function of temperature therefore leads to absolute bounds on the wave attenuation, shown in Fig. 4(c). Below about 500 mK, the effect of wave damping is very small, and it becomes advantageous to use a propagation method.

The procedure then is to create waves with an ac signal $V_{\rm ac}e^{-i\omega t}$ applied to IDC A, over which a height d_A of helium is set by a bias voltage $V_{\rm dc}^A$. These propagate over IDC B $[d_B, V_{\rm dc}^B]$ onto IDC C $[d_C, V_{\rm dc}^C]$, where they are detected as a time-varying capacitance $C(t)$. Because the receiver is biased, $C(t)$ induces a charge variation proportional to $V_{\rm dc}^A V_{\rm dc}^C V_{\rm ac} e^{i(kL_{\rm eff}-\omega t)}$, where $L_{\rm eff} = (L_A + 2L_B + L_C)/2$ is the effective propagation length from A to C in the low damping limit. To observe such a signal, the transmitter A and the receiver C must have the same resonance condition $(d_A = d_C; V_{\rm dc}^A = V_{\rm dc}^C)$. The depth d_B can be set independently.

Figure 4(a) displays a signal obtained by sweeping the driving frequency at fixed bias voltages, using phase sensitive detection on C referenced to the excitation on A. Writing $k = k' + ik''$, we expect the detected amplitude to vary as $\cos(k'L_{\rm eff})\exp(-k''L_{\rm eff})$. The dephasing due to k' produces the expected frequency interval between maxima $(\delta k L_{\rm eff} = 2\pi)$ of $\delta\nu = 3\nu\lambda/2L_{\rm eff}$ for large depths.

Figure 4(b) shows the peak signal amplitude $S(T)$ for $d \sim 1$ μm and $\lambda = 10$ μm. The attenuation factor $k''(T)$ can be deduced using $S(T)/S(T_M) = \exp -[k''(T) - k''(T_M)]L_{\rm eff}$, aside from an additive constant $k''(T_M)$. For convenience, the reference temperature

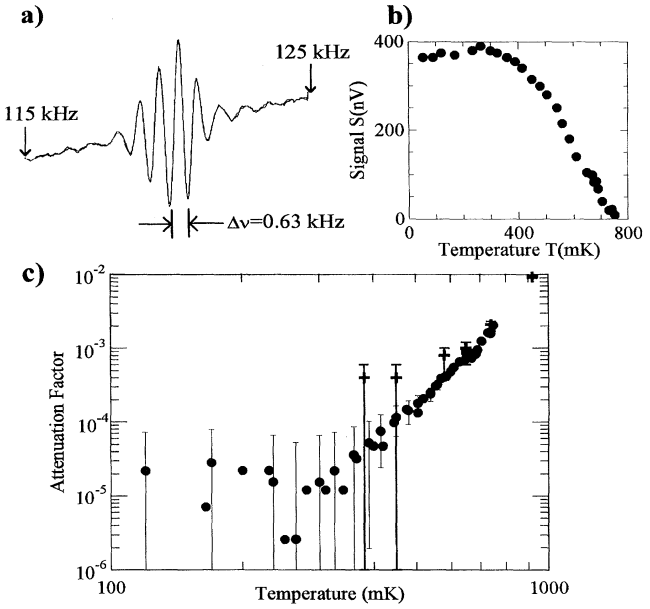

FIG. 4. (a) In-phase signal received by structure C vs frequency of excitation applied to structure A, due to the propagation of a capillary wave. $V_{\rm dc}^A = V_{\rm dc}^C = 128$ V, $V_{\rm dc}^B = 290$ V, $T = 200$ mK. (b) Peak signal height vs temperature at constant excitation for $\lambda = 10$ μm. The maximum corresponds to a wave amplitude $\zeta(k) \sim 100$ Å. (c) Attenuation factor k''/k' (where $k = k' + ik''$), for $\lambda = 10$ μm in the bulk limit $k'd > 1$. (●) Obtained from the data of (b), with the value $k''(T_M)/k' = 1 \times 10^{-6}$ estimated from a fit to $k'' = AT^\nu$. (+) Bounds obtained from emitter resonance linewidths, making no assumptions about structure quality.

is chosen to correspond to the maximum observed signal, $T_M \sim 300$ mK; the reduction below T_M is not thought to be intrinsic to the ripplons [15].

An upper bound for the minimum observed attenuation $k''(T_M)/k' \leq 3 \times 10^{-4}$ is set by resonance linewidths. A further refinement may be made at the price of hypothesizing power-law behavior, $k'' = AT^\nu$, as predicted by all current theories. A best fit for $T_M < T < 700$ mK yields $k''(T_M)/k' \sim 1 \times 10^{-6}$. This represents an insignificant correction for the majority of the data. Figure 4(c) shows the values of $k''(T)$ deduced.

All the results on damping are displayed in Fig. 5. The data are all compatible with power-law behavior for $300 < T < 700$ mK, with $\nu = (4.5 \pm 1)$. Although there is a clear trend with wave number, the range is insufficient to deduce a functional dependence. The dramatic, but inescapable result is that the absolute value is 6 orders of magnitude *lower* than the predictions of established theory [8–10].

Theoretical reevaluation of the damping.—Saam's quantum theory for damping from the three-ripplon interaction, based on inviscid hydrodynamics, has been reexamined in the light of this flagrant discordance [11].

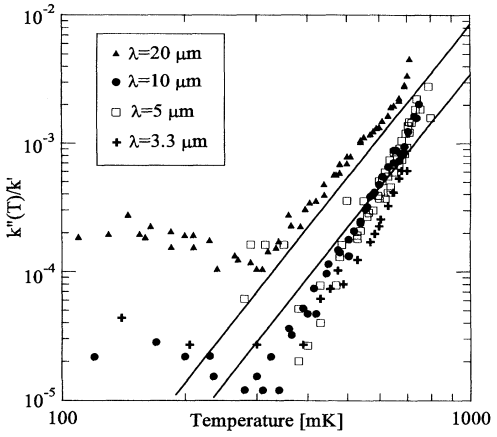

FIG. 5. Attenuation factor $k''(T)/k'$ deduced from propagation measurements for a sequence of wavelengths $3.3 < \lambda < 20\ \mu$m the bulk limit $kd > 1$. The reference attenuation $k''(T_M)$ (see text) is eliminated by hypothesizing $k''(T) = AT^{\nu}$; within this procedure, errors are $\sim 5 \times 10^{-5}$. The upper and lower lines are the new theoretical predictions for $\lambda = 20\ \mu$m and $\lambda = 3.3\ \mu$m, respectively.

The neglect of curvature in applying the surface boundary condition had led to missing a term that almost exactly cancels the one retained. In fact, the dominant effect is the ripplon-two-phonon interaction, were phonons are reflected and Doppler shifted from surface ripples. It leads to Stefan-Boltzmann-like result for ripplons of wave number k,

$$\frac{k''}{k'} \approx \frac{\pi^2}{90}\frac{\hbar k}{\rho\omega}\left(\frac{k_B T}{\hbar s}\right)^4, \tag{4}$$

where s is the sound velocity. The new prediction is shown in Fig. 5, whereas the original three-ripplon calculation is 6 orders of magnitude stronger and the corrected three-ripplon result 6 orders of magnitude weaker.

We reassuringly conclude that, despite initial alarms, quantum hydrodynamics does give a good description of ripplon damping.

We are grateful to Claudine Chaleil for making the interdigital capacitors. The participation of N.J.A. was made possible by a grant from the European Commission Human Capital and Mobility Program (Contract No. ERBCHRXCT930374).

[1] D. O. Edwards and W. F. Saam, *Progress in Low Temperature Physics,* edited by D. F. Brewster (North-Holland, Amsterdam, 1978), Vol. VII A, p. 263.
[2] K. A. Pickar and K. R. Atkins, Phys. Rev. **178**, 399 (1969).
[3] P. J. King and A. F. G. Wyatt, Proc. R. Soc. London A **322**, 355 (1971).
[4] S. Consolo and G. Jacucci, in *Proceedings of the Conference on Low Temperature Physics, LT-13,* edited by K. D. Timmerhaus, W. J. O'Sullivan, and E. F. Hammel (Plenum, New York, 1974), Vol. I, p. 337.
[5] W. F. Vinen, N. J. Appleyard, L. Skrbek, and P. K. H. Sommerfeld, Physica (Amsterdam) **197B**, 360 (1994).
[6] C. C. Grimes and G. Adams, Phys. Rev. Lett. **42**, 795 (1979).
[7] G. Deville, J. Low Temp. Phys. **72**, 135 (1988).
[8] W. F. Saam, Phys. Rev. A **8**, 1918 (1973).
[9] H. Gould and V. K. Wong, Phys. Rev. B **18**, 2124 (1978).
[10] R. C. Jones, A. J. E. Williams, W. F. Vinen, and P. A. Ewbank, J. Low Temp. Phys. **92**, 239 (1993).
[11] P. Roche, M. Roger, and F. I. B. Williams (to be published).
[12] L. D. Landau and E. M. Lifshitz, *Electrodynamics of Continuous Media* (Pergamon Press, New York, 1966), Sec. 15.
[13] B. A. Auld, *Acoustic Fields Waves in Solids* (John Wiley and Sons, New York, 1973), Vol. II, Sec. 10.
[14] The capillary rise experiment of H. M. Guo, D. O. Edwards, R. E. Sarwinski, and J. T. Tough, Phys. Rev. Lett. **27**, 1259 (1971), gives $\sigma = 0.378 \pm 0.002$ mJ m^{-2}, whereas the long wavelength capillary-gravity wave frequency approach of M. Iino, M. Suzuki, and A. J. Ikushima, J. Low Temp. Phys. **61**, 155 (1985), gives $\sigma = 0.3544 \pm 0.0005$ mJ m^{-2}.
[15] The signal appears to be coupled to a low frequency mode excited by ambient vibrations. The signal output showed increasingly strong fluctuations at $\sim$ 5 Hz as T fell below T_M. Artificially exciting this mode by modulating $V_{\rm dc}^B$ reduced the average value of S; the quality factor of the mode, and with it the magnitude of its effect, increased with decreasing temperature. Increasing ^{3}He concentration from 10^{-8} to 10^{-5} had no effect.